Preparation, structure and magnetic properties of synthetic ferrihydrite nanoparticles

IOP Conf. Series: Journal of Physics: Conf. Series **994** (2018) 012003 doi:10.1088/1742-6596/994/1/012003

Preparation, structure and magnetic properties of synthetic ferrihydrite nanoparticles

S V Stolyar[1,2], R N Yaroslavtsev[1,2], O A Bayukov[2], D A Balaev[1,2], A A Krasikov[2], R S Iskhakov[2], A M Vorotynov[2], V P Ladygina[3], K V Purtov[4], M N Volochaev[2]

[1]Siberian Federal University, Krasnoyarsk, 660041, Russia
[2]Kirensky Institute of Physics, SB RAS, Krasnoyarsk, 660036, Russia
[3]International scientific centre for organism extreme states research attached Presidium of KSC, SB RAS, Krasnoyarsk, 660036, Russia
[4]Institute of Biophysics, SB RAS, Krasnoyarsk, 660036, Russia

rauf@iph.krasn.ru

Abstract. Superparamagnetic ferrihydrite powders with average nanoparticle sizes of 2.5 nm produced by the chemical deposition method. Static and dynamic magnetic properties are measured. As a result of ultrasonic treatment in the cavitation regime of suspensions of ferrihydrite powders in a solution of the albumin protein, the Fe ions are reduced to the metallic state. A sol of ferrihydrite nanoparticles is prepared in an aqueous solution of arabinogalactan polysaccharide.

1. Introduction

Fine powders (powders with particle sizes less than 10 nm) based on oxides, hydroxides, and oxyhydroxides of iron are the object of increased interest at the present time.This circumstance is due to the practical use of powders in such areas as catalysis, biomedicine, etc. [1]. Bulk ferrihydrite is an antiferromagnet. However, as the particle sizes decrease to nanoscale, the magnetic properties of the powder change radically. Nanoparticles of ferrihydrite acquire a constant magnetic moment due to incomplete compensation of the magnetic moments of the sublattices. Another important practical feature of ferrihydrite is its absolute biocompatibility, because this mineral is the core of the ferritin protein complex, which is the main carrier of iron in all higher living organisms. Therefore, ferrihydrite powders can compete with powders of conventional ferro- and ferrimagnets used in various practical applications [2], including for targeted drug delivery, as well as for contrasting in magnetic resonance imaging [3].

A method for obtaining stable sols of ferrihydrite nanoparticles of biogenic origin was developed in [4] (ferrihydrite nanoparticles are formed on the cell surface during the cultivation of Klebsiella oxytoca bacteria). As it turned out, the magnetic properties of biogenic nanoparticles of ferrihydrite can be modified by heat treatment [5], however, it is not possible to produce a stable sol on the basis of annealed powders. As a matrix for the preparation of stable sols based on chemically produced ferrihydrite powders, it is possible to use organic preparations such as water-soluble proteins albumin or natural polysaccharide arabinogalactan.

The aim of this work was the production of ferrihydrite powders and finding ways to preparation of sols based on them. The process of preparation of ferrihydrite-based sols consists in the ultrasonic treatment of suspensions of nanoparticles.

2. Experimental methods

Synthetic ferrihydrite nanoparticles were prepared chemically [6]. At room temperature and constant stirring, a 1 M alkali solution of NaOH was added to a 0.2 M solution of iron nitrate $Fe(NO_3)_3 \cdot 9H_2O$ to a neutral pH value. The precipitate formed was collected on a filter. Then, the precipitate was washed and dried at room temperature. The electron microscopy examination was carried out on a Hitachi HT7700 transmission electron microscope. The Mössbauer spectra were measured on an MS-1104Em spectrometer with a $^{57}Co(Cr)$ source. The chemical isomer shifts were given with respect to α-Fe. The magnetic measurements were carried out on a vibrating-sample magnetometer [7]. The temperature dependences of the magnetic moment M(T) were measured both in the mode of cooling without a magnetic field (zero field cooling (ZFC)) and in the mode of cooling in an external magnetic field (field cooling (FC)). The magnetic resonance spectra were recorded on a Bruker ELEXSYS 560 spectrometer operating in the X band mode (the characteristic microwave radiation frequency was ~9.4 GHz) at temperatures in the range from 100 to 300 K. Ultrasonic treatment was performed on the Volna UZTA-0.4/22-OM apparatus. The intensity of ultrasonic treatment was over 10 $W \cdot cm^{-2}$ and the frequency was 22 kHz. The treatment time was 4–24 min. Ultrasonic treatment was carried out in an aqueous medium, in a solution of protein albumin and arabinogalactan.

3. Results and discussion

Figure 1 shows the results of transmission electron microscopy of the obtained ferrihydrite nanoparticles. Figure 1 (a) shows the microdiffraction pattern of nanoparticles, which is characteristic of ferrihydrite nanoparticles [8,9]. Two diffuse reflections with interplanar distances d_1 = 1.6 Å, d_2 = 2.7 Å are observed. The average particle size was D = 2.5 nm (Fig. 1 (b)).

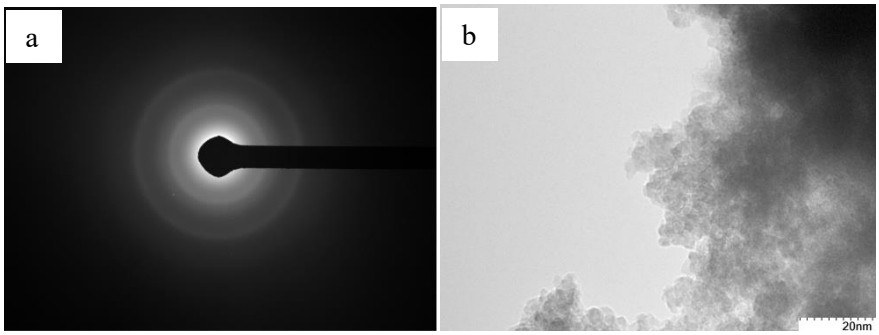

Figure 1. Microdiffraction of ferrihydrite nanoparticles (a), transmission electron microscope images (b).

The temperature dependences of the magnetization, measured in the ZFC and FC modes, shown in Fig. 2a, exhibit a characteristic superparamagnetic (SP) behavior. At $T < T_B$, the *M(H)* curves exhibit a hysteresis, see the inset of the fig.2.a Analysis of the *M(H)* dependences at temperatures $T > T_B$ (see the fig.2b) was carried out using the standard approach for systems of noninteracting antiferromagnetic nanoparticles. In this approach, the magnetic moment of the sample is determined by the SP behavior of individual particles, taking into account their distribution over magnetic moments, and also the $\chi_{AF} \cdot H$ component, which determines the antiferromagnetic contribution to the magnetization. In this case, the *M(H)* dependences are described by the following expression [7,10,11]:

$$M(H) = N_P \int_{\mu_{min}}^{\mu_{max}} L(\mu_P, H) f(\mu_P)\, \mu_P d\mu_P + \chi_{AF} \cdot H. \quad (1)$$

In this expression $L(\mu_P, H)$ – Langevin function, $f(\mu_P)$ – distribution function of the magnetic moment of the particles μ_P, N_P – number of particles per unit weight of the sample. The lognormal distribution was used [10]. From the temperature dependence $\langle\mu_P\rangle(T)$, by extrapolation to $T = 0$ K, values of $\langle\mu_P\rangle(T = 0)$ were determined, which amounted to 173 μ_B. The fig.2b shows experimental isotherms of magnetization $M(H)$ as well as the results of the best fit using eq.(1) and partial contributions of the first (superparamagnetic) and the second (antiferromagnetic $\chi \cdot H$) terms of eq.(1).

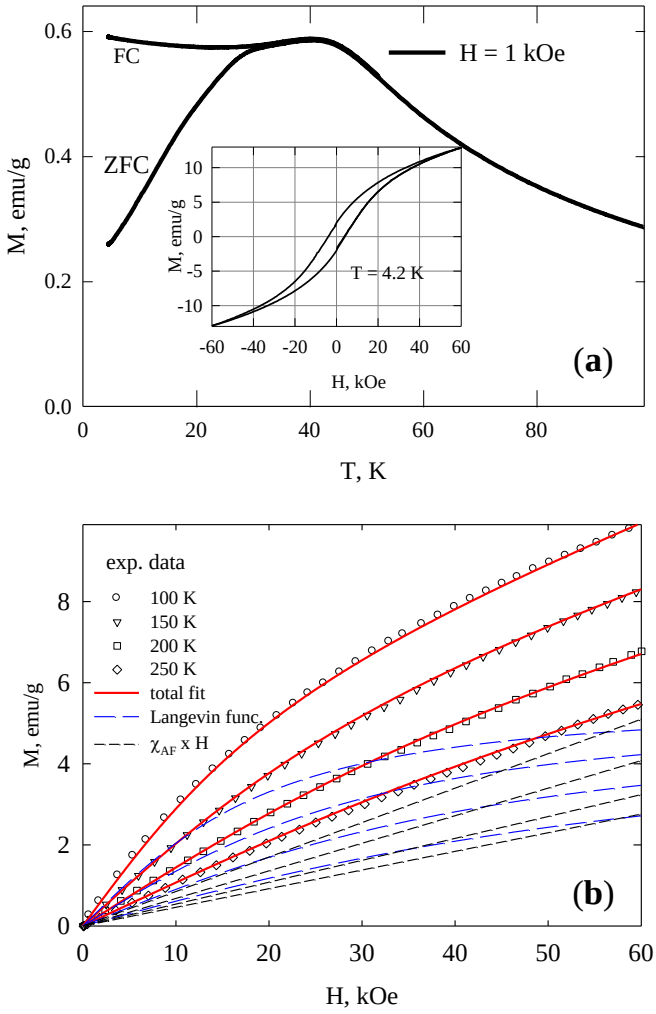

Figure 2. Magnetic properties of synthetic ferrihydrite nanoparticles. (a) The temperature dependences of the magnetic moment M(T) measured in the ZFC and FC modes. Inset in fig.2(a) – hysteresis dependence $M(H)$ at T = 4.2 K. (b) –Magnetization curves $M(H)$ obtained at different temperatures and the results of the best fit using eq.(1). Partial contributions of superparamagnetic antiferromagnetic $\chi \cdot H$ terms of eq.(1) are also shown.

Table 1 shows the values of the particle size D, the blocking temperature T_B, the coercive field H_C, the saturation magnetization M_S and the antiferromagnetic susceptibility χ_{AF}. For comparison, the table also shows the characteristics of ferrihydrite nanoparticles obtained as a result of cultivation of bacteria [12].

Table 1. Characteristics of the ferrihydrite samples

Sample	D, nm	T_B, K	H_C, kOe	M_s, Gs	χ_{AF}, 10^{-4} emu/(g·Oe)
Biogenic [5,7]	2	23.3	3.6	26	0.6
Synthetic	2.5	40	3.8	25	1.1

Ferromagnetic resonance spectra of ferrihydrite nanoparticles are symmetrical curves of the Lorentz shape, and the absorption maximum is located near ω/γ value, which for a given frequency is 3350 Oe. For ferrihydrite nanoparticles in the investigated temperature range, the intensity of the FMR signal decreased linearly, indicating that the nanoparticles are in the unlocked, SP state.

According to the Raikher-Stepanov theory [13,14], in the powders of randomly oriented particles of ferromagnets and ferrites, the width of the absorption line is a nonmonotonic function of temperature:

$$\Delta\mathrm{H(T)} = \Delta H_S(T) + \Delta H_U(T), \qquad (2)$$

where $\Delta H_S(T)$ – contribution to the broadening due to superparamagnetism of nanoparticles, $\Delta H_U(T)$ – contribution to the broadening due to the scatter in the directions of the anisotropy fields of the particles (inhomogeneous broadening), which is decisive at low temperatures.

Figure 3 shows the values of the width of the FMR line as a function of temperature and the result of fitting of experimental data using the Raikher-Stepanov theory. The curve shown in Figure 3 is characterized by two adjustable parameters: *KV* and *MV*. Table 2 shows the values obtained, as well as *KV* and *MV* of nanoparticles of ferrihydrite of biogenic origin. The table also shows the corresponding parameters of ferritin complexes calculated from the temperature curves of FMR [15].

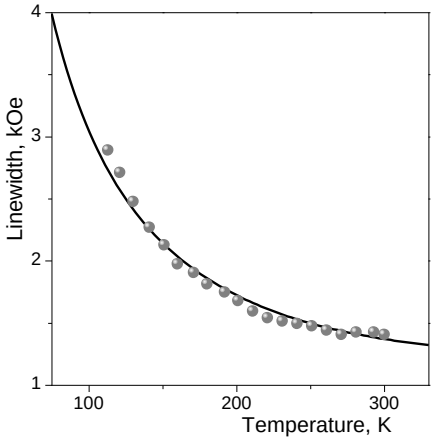

Figure 3. Temperature dependences of the width of the ferromagnetic resonance line for ferrihydrite nanoparticles. The solid line is the result of the fit.

Table 2. Fitting parameters of $\Delta H(T)$curves

Sample	*KV*, erg	*MV*, emu
Biogenic	$1.25\cdot10^{-14}$	$2.37\cdot10^{-18}$
Synthetic	$2\cdot10^{-14}$	$2.4\cdot10^{-18}$
Ferritin[15]	$2.5\cdot10^{-14}$	$1.9\cdot10^{-17}$

Figure 4 (curve 1) shows the Mossbauer spectrum of chemically prepared ferrihydrite nanoparticles, characterized by a paramagnetic doublet. Table 3 shows the results of the interpretatation. Three main non-equivalent positions of Fe^{3+} ions having octahedral coordination are registered: positions Fe1 and Fe2 with a relatively small degree of distortion of local symmetry and position of Fe3 with a large degree of distortion. After ultrasonic treatment of nanoparticles in water (curve 2), no significant changes in Mossbauer parameters were observed except for some redistribution in octahedral positions of Fe. Figure 4 also shows the Mössbauer spectrum of nanoparticles after ultrasonic treatment in an albumin solution (curve 3). In this case, the spectrum contains an additional sextet. The parameters of the sextet coincide with the Mössbauer parameters of the bcc phase of iron. Thus, ultrasonic treatment in protein solution leads to the reduction of Fe ions to the metallic state (19%).

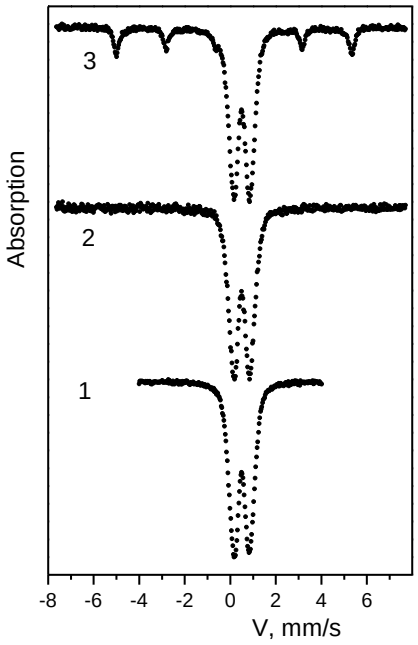

Figure 4. Mossbauer spectra. Initial nanoparticles - 1. After ultrasound treatment in water - 2 and in albumin solution -3.

To obtain the nanoparticle-arabinogalactan complexes, 1% sol of the ferrihydrite particles in distilled water was used. A solution of arabinogalactan (1%) in distilled water was poured onto the sol of the particles in a ratio of 1:1.Homogenization was performed by ultrasound for 10 min using an ultrasonic radiator -UltrasonicdisintegratorUD-20 (Techpan, Poland). The resulting complexes were washed from the excess unbound polysaccharide by centrifuging the particle sol at 35,000 g on a centrifuge Avanti® J-E (Beck-man Coulter, USA). The resulting precipitate was collected and re-homogenized in distilled water. The cycle was repeated 3 times. The final result was a stable sol of the complexes in distilled water, which was used for further research. The resulting complex has the property of restoring, that is, the dried sol particles with the addition of water also form a sol. The possibility of making a sol on the basis of synthetic nanoparticles of ferrihydrite in a solution of albumin was also investigated. The fraction of particles transferred to the sol was insignificant.

Table 3. Mossbauer parameters of ferrihydrite. IS is the isomeric chemical shift, QS is the quadrupole splitting, W is the width of the absorption line, H is the hyperfine field at the iron core, and A is the share population of the position.

	IS, mm/s	H, kOe	QS, mm/s	W, mm/s	A	Position
Initial nanoparticles	0.351		0.51	0.35	0.53	Fe1
	0.355		0.86	0.31	0.37	Fe2
	0.359		1.21	0.26	0.10	Fe3
After ultrasonic in water	0.349		0.49	0.33	0.42	Fe1
	0.352		0.79	0.30	0.38	Fe2
	0.355		1.16	0.33	0.20	Fe3
After ultrasonic in albumin solution	0.006	332	0	0.25	0.19	**α-Fe**
	0.350		0.53	0.35	0.35	Fe1
	0.351		0.84	0.36	0.37	Fe2
	0.357		1.22	0.30	0.10	Fe3

4. Conclusions

Ferrihydrite powders are produced by the chemical deposition method. Static and dynamic magnetic properties are measured. A sol of ferrihydrite nanoparticles is made in an aqueous solution of a natural polysaccharide, arabinogalactan.

Acknowledgments

The reported study was funded by Russian Foundation for Basic Research and Krasnoyarsk region according to the research project № 17-43-240527 and Russian Foundation for Basic Research project № 16-03-00969. Support by the Special Program for Siberian Federal University of the Ministry of Education and Science of the Russian Federation is acknowledged.

References

[1] Tartaj P, Morales M a del P, Veintemillas-Verdaguer S, Gonz lez-Carre o T and Serna C J 2003 The preparation of magnetic nanoparticles for applications in biomedicine *J. Phys. D. Appl. Phys.* **36** R182–97

[2] Dobretsov K, Stolyar S and Lopatin A 2015 Magnetic nanoparticles: a new tool for antibiotic delivery to sinonasal tissues. Results of preliminary studies. *Acta Otorhinolaryngol. Ital. organo Uff. della Soc. Ital. di Otorinolaringol. e Chir. Cerv.-facc.* **35** 97–102

[3] Inzhevatkin E V., Morozov E V., Khilazheva E D, Ladygina V P, Stolyar S V. and Falaleev O V. 2015 Elimination of Iron-Containing Magnetic Nanoparticles from the Site of Injection in Mice: a Magnetic-Resonance Imaging Study *Bull. Exp. Biol. Med.* **158** 807–11

[4] Stolyar S V, Bayukov O A, Balaev D A, Iskhakov R S, Ishchenko L A, Ladygina V P and Yaroslavtsev R N 2015 Production and magnetic properties of biogenic ferrihydrite nanoparticles *J. Optoelectron. Adv. Mater.* **17** 968–72

[5] Balaev D A, Krasikov A A, Dubrovskii A A, Semenov S V., Bayukov O A, Stolyar S V., Iskhakov R S, Ladygina V P and Ishchenko L A 2014 Magnetic properties and the mechanism of formation of the uncompensated magnetic moment of antiferromagnetic ferrihydrite nanoparticles of a bacterial origin *J. Exp. Theor. Phys.* **119** 479–87

[6] Michel F M, Ehm L, Antao S M, Lee P L, Chupas P J, Liu G, Strongin D R, Schoonen M A A, Phillips B L and Parise J B 2007 The Structure of Ferrihydrite, a Nanocrystalline Material *Science (80-.).* **316** 1726–9

[7] Balaev D A, Krasikov A A, Dubrovskiy A A, Popkov S I, Stolyar S V, Bayukov O A, Iskhakov R S, Ladygina V P and Yaroslavtsev R N 2016 Magnetic properties of heat treated bacterial ferrihydrite nanoparticles *J. Magn. Magn. Mater.* **410** 171–80

[8] Kukkadapu R K, Zachara J M, Fredrickson J K, Smith S C, Dohnalkova A C and Russell C K 2003 Transformation of 2-line ferrihydrite to 6-line ferrihydrite under oxic and anoxic conditions *Am. Mineral.* **88** 1903–14

[9] Guyodo Y, Banerjee S K, Lee Penn R, Burleson D, Berquo T S, Seda T and Solheid P 2006 Magnetic properties of synthetic six-line ferrihydrite nanoparticles *Phys. Earth Planet. Inter.* **154** 222–33

[10] Silva N J O, Amaral V S and Carlos L D 2005 Relevance of magnetic moment distribution and scaling law methods to study the magnetic behavior of antiferromagnetic nanoparticles: Application to ferritin *Phys. Rev. B* **71** 184408

[11] Gilles C, Bonville P, Rakoto H, Broto J M, Wong K K W and Mann S 2002 Magnetic hysteresis and superantiferromagnetism in ferritin nanoparticles *J. Magn. Magn. Mater.* **241** 430–40

[12] Stolyar S V., Bayukov O A, Gurevich Y L, Ladygina V P, Iskhakov R S and Pustoshilov P P 2007 Mössbauer study of bacterial ferrihydrite *Inorg. Mater.* **43** 638–41

[13] Raikher Y L and Stepanov V I 1992 Thermal fluctuation effect on the ferromagnetic-resonance line-shape in disperse ferromagnets *JETP* **102** 1409–23

[14] Poperechny I S and Raikher Y L 2016 Ferromagnetic resonance in uniaxial superparamagnetic

particles *Phys. Rev. B* **93** 014441
[15] Wajnberg E, El-Jaick L J, Linhares M P and Esquivel D M S 2001 Ferromagnetic Resonance of Horse Spleen Ferritin: Core Blocking and Surface Ordering Temperatures *J. Magn. Reson.* **153** 69–74